Motor Imagery and Action Observation Induced Electroencephalographic Activations to Guide Subject-Specific Training Paradigm: A Pilot Study

Zhongpeng Wang, *Member, IEEE*, Lu Yang, Mengya Wang, Yijie Zhou, Long Chen, Bin Gu, Shuang Liu, *Member, IEEE*, Minpeng Xu, *Member, IEEE*, Feng He, and Dong Ming, *Senior Member, IEEE*

***Abstract*— Brain-computer interface (BCI)-based motor rehabilitation feedback training system can facilitate motor function reconstruction, but its rehabilitation mechanism with suitable training protocol is unclear, which affects the application effect. To this end, we probed the electroencephalographic (EEG) activations induced by motor imagery (MI) and action observation (AO) to provide an effective method to optimize motor feedback training. We grouped subjects according to their alpha–band sensorimotor cortical excitability under MI and AO conditions, and investigated the EEG response under the same paradigm between groups and different motor paradigms within group, respectively. The results showed that there were significant differences in sensorimotor activations between two groups of subjects. Specifically, the group with weaker MI induced EEG features, could achieve stronger sensorimotor activations in AO than that of other conditions. The group with stronger MI induced EEG features, could achieve stronger sensorimotor activations in the MI+AO than that of other conditions. We also explored their classification and brain network differences, which might try to explain the EEG mechanism in different individuals and help stroke patients to choose appropriate subject-specific motor training paradigm for their rehabilitation and better treatment outcomes.**

***Index Terms*— Brain–computer interface, motor imagery, action observation, electroencephalographic activations, motor feedback training.**

Manuscript received 5 August 2022; revised 15 December 2022 and 10 March 2023; accepted 9 May 2023. Date of publication 12 May 2023; date of current version 30 May 2023. This work was supported in part by the National Key Research and Development Program of China under Grant 2022YFF1202304; in part by the National Natural Science Foundation of China under Grant 62006171, Grant 81925020, and Grant 82001939; and in part by the Natural Science Foundation of Tianjin under Grant 20JCYBJC00930. *(Corresponding authors: Long Chen; Dong Ming.)*

This work involved human subjects or animals in its research. Approval of all ethical and experimental procedures and protocols was granted by Ethics Committee of Tianjin University.

Zhongpeng Wang, Minpeng Xu, Feng He, and Dong Ming are with the Academy of Medical Engineering and Translational Medicine, Tianjin University, Tianjin 300072, China, also with the College of Precision Instruments & Optoelectronics Engineering, Tianjin University, Tianjin 300072, China, and also with the Tianjin International Joint Research Center for Neural Engineering, Tianjin 300072, China (e-mail: richardming@tju.edu.cn).

Lu Yang, Yijie Zhou, Long Chen, and Shuang Liu are with the Academy of Medical Engineering and Translational Medicine, Tianjin University, Tianjin 300072, China, and also with the Tianjin International Joint Research Center for Neural Engineering, Tianjin 300072, China (e-mail: cagor@tju.edu.cn).

Mengya Wang and Bin Gu are with the College of Precision Instruments & Optoelectronics Engineering, Tianjin University, Tianjin 300072, China.

Digital Object Identifier 10.1109/TNSRE.2023.3275572

I. Introduction

STROKE is a combination of local or global brain dysfunction caused by an unexpected vascular lesion in the brain area. It is the first disabling malignant nervous system disease in China and even in the world, with high incidence, disability and recurrence [1], [2], [3]. The most common and widely known dysfunction in stroke patients is limb movement disorder, which in most cases affects the motor control of the face, arms and legs on one side of the body, called hemiplegia [4]. Common motor function problems in hemiplegia include muscle weakness, spasticity, increased reflexes, loss of coordination, and apraxia. Impaired limb function largely limits the patient's ability to perform daily activities [5], severely affecting his or her normal life [6], and effective rehabilitation aids are urgently needed [7], [8], [9], [10].

Traditional rehabilitation training involves passive movement of the hemiplegic limb with the help of a physical therapist to promote muscle strength recovery and motor nerve reconstruction to restore the motor function of the limb [11], [12]. However, such passive rehabilitation does not motivate patients to participate in training [13] and is not sufficient to produce effective plasticity in the cerebral motor cortex [14]. Although there are innate repair mechanisms in the central nervous system after stroke [15], its endogenous regeneration ability is limited [16]. Therefore, it is necessary to use sports rehabilitation training to promote the recovery of motor function after stroke. The motor feedback training based on Brain-computer Interface (BCI) provides a new idea for the rehabilitation of motor function, making the process of motor rehabilitation training observable, quantifiable and self-adjustable [17], [18].

The BCI-based motor rehabilitation feedback training system can drive the external equipment to produce movement

on the injured limb according to the patient's subjective motor intention and achieve the simultaneous activation of the central nervous system and peripheral nervous system, thus effectively promoting the recovery of motor function of stroke patients [19], [20], [21]. However, there are problems such as unclear rehabilitation mechanisms with suitable training protocol at present, which limit the the application effect of the system [22]. MI and AO are two main types of motor evoked paradigms that are considered as promising tools for motor rehabilitation [23]. Studying their related rehabilitation mechanisms can help stroke patients choose their own motor evoked paradigms in motor rehabilitation, so that patients can get better therapeutic effects. MI refers to the preview of motor behavior in the brain, which belongs to the hidden phase of motor intention [24], [25]. AO is the conscious and structured observation of human movement [26].

During imagination and observation, the brain retrieves motor events with similar characteristics from a library of motor instructions and mobilizes motor-related cortex to mentally imitate the imagined or observed movements, thereby facilitating motor function recovery in the injured limb [22]. Gatti R et al. revealed that AO as a novel strategy for learning complex motor tasks is superior to MI in the early stages of motor learning [27]. Taube W et al. explored cortical activation in MI, AO and AO+MI conditions, respectively. fMRI imaging results showed that MI elicited bilateral activation in the supplementary motor area, shell nucleus and cerebellum, and AO+MI activated ventral and dorsal premotor cortex and primary motor cortex, but no significant activation was found in the supplementary motor cortex, premotor cortex, primary motor cortex and cerebellum in the AO condition [28]. Clark S et al. investigated the differential excitability of the corticospinal tract in MI and AO conditions, respectively, evaluating metrics using MEPs evoked by transcranial magnetic stimulation. The findings suggested that both conditions produced similar facilitation on MEPs [29]. That said, there are no consistent results from the current studies on MI and AO in terms of promoting early motor learning and motor cortex activation effects. Therefore, it is important to investigate the causes of the differences in EEG activation induced by MI and AO to help stroke patients choose the appropriate motor evoked paradigm for their motor rehabilitation, so that they can achieve better treatment outcomes.

We grouped the subjects according to the individual differences of EEG activation induced by AO and MI, and compared the EEG response characteristics of the two groups to find the main reasons for this difference. We also explored classification and brain network differences of MI and AO, which might try to explain EEG mechanism in different individuals and choose the appropriate motor evoked paradigm for stroke patients in the motor rehabilitation feedback training, so as to provide theoretical basis and experimental support for shortening the rehabilitation process and obtaining better treatment effects.

II. Methods

A. Subjects

The study was conducted in the Neural Engineering and Rehabilitation Laboratory of Tianjin University and all experiments were approved by the Ethics Committee of Tianjin University. A total of 26 healthy subjects participated our experiments, all of whom were graduate students at Tianjin University, and 13 of them were female. The age range of the subjects was 20-28 years old, with a mean age of 23.8 $\pm$ 1.7 years. All subjects did not have any history of neurological disease and had normal or corrected-to-normal visual acuity. Each subject was clearly informed about the experimental procedure and signed a written informed consent form before recording the data.

B. Experimental Paradigm

We investigated the differences in EEG activations under different motor evoked paradigms. For this purpose, the experiment was designed with three experimental tasks, AO, MI, and MI+AO. In the AO condition, subjects were only required to observe the right hand grasp video during the task period. In the MI condition, subjects were asked to imagine the same right hand grasp action as in the video with textual cues. In the MI+AO condition, subjects were not only required to watch the video, but also to follow the video to imagine the corresponding action. The time to complete a right-handed grasp in the video was 1s. Before the experiment, subjects were asked to watch the video in advance to become familiar with the action to be observed and imagined, and to adapt to the frequency of the hand grasp in the video so as to better complete the experimental task.

In the experiment, the subjects were allowed to sit in a chair in a comfortable manner of their choice and keep their hands relaxed. Each experiment consisted of 3 sessions, each session contained 40 trials and corresponded to one experimental condition. The experimental paradigm for each session is shown in Fig. 1. Each trial lasted 8 s, including 4 s of rest, 1 s of preparation, and 3 s of task period. The experiment started with a white circle in the center of the screen, which has lasted 4 s, during which the subject was asked to relax and rest. The white circle then turned red and lasted for 1s, prompting the subject to enter the MI preparation phase. After this period, the red circle disappeared and the monitor presented a 3 s video of a right-handed grasp, for a total of 3 grasps during the task period. In the MI condition, the monitor no longer showed the grasp video during the task period, but displayed the words "please imagine" for the same duration of 3 s, during which the subject was asked to imagine the right-hand grasp three times. During the experimental phase, subjects were asked to refrain from physical movements and to minimize blinking during the imagery task to ensure the stability of the collected EEG data.

C. EEG Signal Acquisition and Preprocessing

Experiments were performed using the 64-channel SynAmps2 EEG amplifier system (Neuroscan, Australia) and its accompanying 64-channel Quik-Cap electrode cap to acquire EEG signals from the subjects. The electrodes are made of Ag/AgCl and are positioned according to the international standard 10-20 system, where the overhead electrode located between CZ and CPZ is the reference electrode and the forehead GND is used as ground. The sampling rate

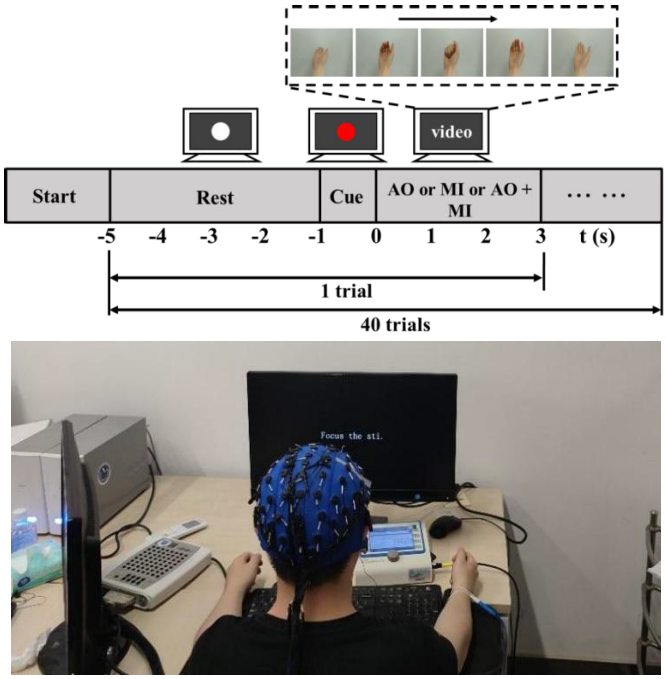

Fig. 1. Experimental setup. Schematic diagram of the experimental paradigm for each session and experimental scene diagram.

is 1000 Hz and the bandwidth is 0.5-100 Hz. In addition, a 50 Hz trap filter is used to filter out industrial frequency interference. During EEG signal acquisition, the impedance of each electrode is kept below 20 kΩ.

To pre-process the raw signal, the EEG with an original sampling rate of 1000 Hz was first downsampled to 200 Hz. Subsequently, the downsampled EEG signal was filtered with a 3rd order Butterworth bandpass filter in the frequency range of 5-35 Hz to remove artifacts. The EEG data were processed during the experiments using the EEGLAB toolbox in MATLAB. EEGLAB, developed by the Swartz Center for Computational Neuroscience Research at the University of California, San Diego, is a MATLAB toolbox for processing multichannel EEG signals. Users can process EEG data through menu options in the GUI or write custom data processing scripts through functions in EEGLAB [30].

D. Event-Related Spectral Perturbation Analysis

During MI and AO, neurons in the relevant cortex of the brain generate synchronized oscillatory activity, which is macroscopically manifested as ERD/ERS phenomena, mainly in the alpha and beta (8-14 Hz and 15-28 Hz) frequency bands. In order to investigate the energy changes of EEG signals in subjects under different experimental conditions, we used the Event-related Spectral Perturbation (ERSP) method to analyze the EEG signals in the time-frequency domain. The ERSP method averages the power spectrum in a short sliding time window over multiple trials, and then presents the ERD/ERS patterns corresponding to different task states [31]. They represent the average power spectrum changes of the EEG signal in response to the stimulus. They are defined by the formula [30]:

$$\mathrm{ERSP}(f,t) = \frac{1}{n}\sum_{k=1}^{n}\left(F_k(f,t)^2\right) \tag{1}$$

where n denotes the number of experimental trials, and $F_k(f,t)$ denotes the the spectral estimate of the kth trial at a particular frequency f and time t. In this experiment, the ERSP values of the key channels C3, FC3, and CP3 corresponding to the sensorimotor cortex, premotor cortex, and supplementary motor cortex were analyzed.

Widespread low-alpha and low-beta band desynchronization is associated with increased levels of attention and motor system arousal during motor execution and action observation. In contrast, high alpha and high beta band desynchronization reflects the activation of neural circuits associated with individual processing of motor commands and somatosensory and visual feedback during motor execution and action observation [32]. To investigate the differences in EEG response characteristics of subjects under different experimental conditions throughout the task period, the average ERD values were calculated in four frequency bands: low alpha band (8-10 Hz), high alpha band (10-14 Hz), low beta band (15-20 Hz) and high beta band (20-28 Hz).The ERD values were calculated as shown in (2):

$$ERD_{valve} = \frac{1}{N}\sum_{f\in F}\sum_{t\in T}(ERSP(f,t)) \tag{2}$$

where F denotes the frequency band to be calculated, T denotes the length of the selected task period, and N refers to the number of all time-frequency points within the selected band time range. The ERSP values of 60 channels (with CB1, CB2, M1, and M2 removed) were used to construct the brain topography in this experiment.

Higher significance (reactivity) of frequency components in the alpha as compared to the beta range during imagination of hand movement was also reported previously [33], [34]. In general, the energy drop of subjects in the high alpha band is more obvious than that in the low alpha band. And C3 channel is usually often selected in the study of MI [33], [35]. Therefore, after calculating the mean ERSP values under the four frequency bands during the task, the subjects were divided into two groups according to the ERD values in the high alpha frequency band (10-14 Hz) of C3 channel under MI and AO conditions. Group 1 (12 subjects): subjects with stronger MI-evoked ERD characteristics than AO. Group 2 (14 subjects): subjects with weaker MI-evoked ERD characteristics than AO. We investigated the cortical EEG activation under the same evoked paradigm between groups and different motor evoked paradigms within the group, respectively.

E. PDC Based Functional Connectivity Analysis

Functional connectivity partly reflects potential interactions between brain regions [36]. Functional connectivity between brain regions can be analyzed using Partial Directed Coherence (PDC). Partial Directed Coherence provides a clearer and more direct frequency domain connectivity map of Granger causality compared to Directed Coherence, especially when more than two time series are analyzed simultaneously [37]. The specific calculation process is as follows:

For the multi-channel autoregressive model, it could be expressed as follows:

$$\begin{bmatrix} x_1(n) \\ x_2(n) \\ \vdots \\ x_m(n) \end{bmatrix} = \sum_{i=1}^{p} C_i \begin{bmatrix} x_1(n-i) \\ x_2(n-i) \\ \vdots \\ x_m(n-i) \end{bmatrix} + \begin{bmatrix} w_1(t) \\ w_2(t) \\ \vdots \\ w(t) \end{bmatrix} \quad (3)$$

In formula (3):

$$C_i = \begin{bmatrix} c_{11i} & c_{12i} & \cdots & c_{1mi} \\ c_{21i} & c_{22i} & & c_{2mi} \\ \vdots & & \ddots & \vdots \\ c_{m1i} & c_{m2i} & \cdots & c_{mmi} \end{bmatrix}$$

The brain network analysis of this experiment involved 38 channels of EEG signals, corresponding to $m = 38$. According to the EEG signals of 38 channels, the parameters of formula (3) were obtained and Fourier transformed, and the transformed formula was shown in formula (4):

$$\mathrm{A}(f) = \sum_{i=1}^{p} C_i e^{-j2\pi i f/fs} \quad (4)$$

$$\bar{A}(f) = I - \sum_{i=1}^{p} C_i e^{-j2\pi i f/fs} \quad (5)$$

where I is identity matrix, and its dimension is $m = 38$. Finally, the partial directed coherence of $x_j \rightarrow x_k$ was calculated by formula (6):

$$PDC_{x_j \rightarrow x_k}(f) = \frac{\overline{a_{k,j}}(f)}{\sqrt{\sum_{i=1}^{m} \left|\overline{a_{i,j}}(f)\right|^2}} \quad (6)$$

In formula (6), $\overline{a_{k,j}}(f)$ refers to the j element in the k row in matrix $\bar{A}(f)$, and $\overline{a_{i,j}}(f)$ refers to the j element in the i row in matrix $\bar{A}(f)$. The range of the normalized $PDC_{x_j \rightarrow x_k}(f)$ is [0, 1], which indicates the proportion of this information flowing to x_k in all the information flows from x_j. If the proportion is greater than the set threshold, it is considered that there is a connection between the two channels. If the proportion is less than the threshold, it is determined that there is no connection between the two channels. The final PDC value is a 38 × 38 matrix, and the elements in the matrix reflect the intensity and direction of information flow between each channel.

A directed weighted brain network map can be constructed by calculating the resulting PDC values. After drawing the brain network topology of the subjects under different task conditions, the characteristics of the brain network are analyzed using parameters such as causal flow. A higher value of causal flow indicates a greater causal influence of the node on the whole system.

F. Classification

To investigate the difference in the classification accuracy between the two groups under MI conditions, EEG data from 15 channels (F3, FZ, F4, FC3, FC4, C5, C3, CZ, C4, C6, CP3, CP4, P3, PZ, P4) of sensorimotor cortical were selected to classify the two-class condition of task and resting periods. First, the EEG data of 3 s task period and resting period were intercepted in each trial separately. A 3s data segment was divided into 11 data segments of 2s length by a sliding window with a window width of 2 s and a step size of 0.1 s. So there are 40 trial × 11 = 440 samples in the resting period and 40 trial × 11 = 440 samples in the task period, i.e. 880 samples in total. The EEG data were then divided into training and test sets by a 20-fold cross-validation method (836 samples in the training set and 44 samples in the test set), and the Common Spatial Pattern (CSP) filter and Support Vector Machines (SVM) with a linear kernel were built in the training set and applied to the test set. Finally, 20-fold cross validation was used to calculate the final classification accuracy.

G. Statistical Analysis

The paired and independent sample t-test were used to analyze the mean ERD values generated by subjects under different experimental conditions and the mean ERD values between two groups under the same experimental conditions. The classification accuracy between group 1 and group 2 was also analyzed by t-test. The statistical analysis software used for the experiments was SPSS software (IBM SPSS Statistics, IBM Corporation). The significance level of the statistical test results was set at 0.05.

III. Results and Analysis

A. ERSP Patterns Analysis

Fig. 2 shows the average time-frequency diagrams for group 1 and group 2 subjects in the C3, FC3, and CP3 channels under three experimental conditions (MI+AO, MI, and AO). From the time-frequency diagram of the C3 channel, it could be found that in the alpha and beta bands, a persistent ERD phenomenon was observed during the task period, and under the MI+AO or MI conditions, the subjects in group 1 showed the phenomenon of energy decline during the task period significantly stronger than group 2. In group 1, the high alpha-ERD intensity under MI+AO condition was stronger than that under MI or AO conditions, and the high beta-ERD intensity under MI+AO or MI conditions was significantly stronger than that under AO condition. In group 2, the activation intensity under AO condition was overall stronger than that under MI+AO or MI conditions.

There was a similar phenomenon in the time-frequency diagram of FC3 channel. For example, under MI+AO or MI conditions, subjects in group 1 showed significantly stronger energy decline than in group 2. Activation in group 1 was stronger than group 2 in the alpha band of the AO condition, but the opposite was shown in the beta band. Subjects in group 1 exhibited stronger alpha-ERD phenomena under MI+AO or AO conditions, and stronger beta-ERD phenomena under MI condition. Group 2 showed essentially no persistent ERD phenomenon under MI condition.

There was also a similar phenomenon in CP3 channel. Under MI+AO or MI conditions, group 1 showed significantly stronger energy decline than in group 2. In group 1, the ERD phenomenon was the weakest under the MI condition, and the ERD phenomenon was the strongest under the MI+AO

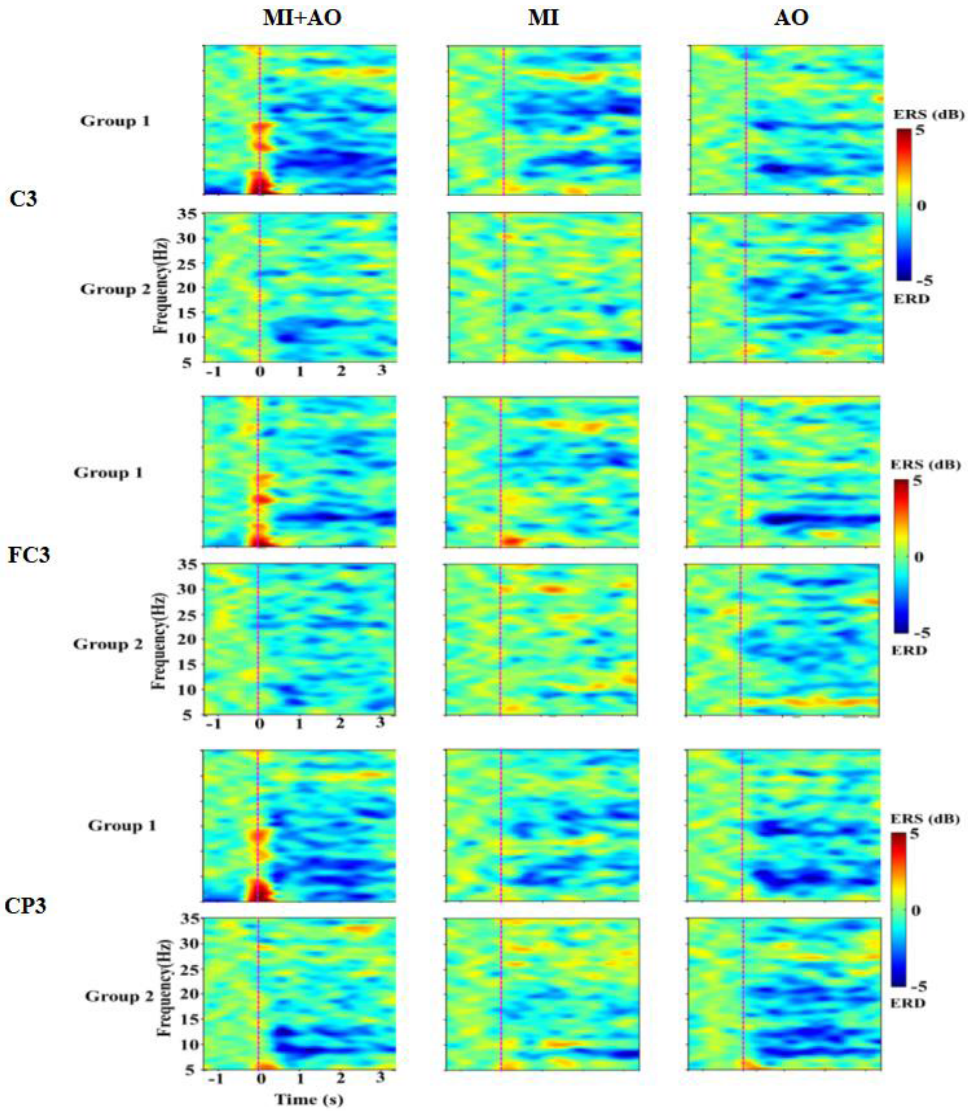

Fig. 2. Average time-frequency diagrams of C3, FC3 and CP3 channels under three experimental conditions. All subplots have the same scale as the first subplot in the second row.

condition. In group 2, the ERD phenomenon under MI condition was the weakest, and the ERD phenomenon under AO condition was the strongest.

In summary, we could find that the ERD phenomenon was stronger in group 1 than in group 2 under MI or MI+AO conditions for either C3, CP3 or FC3 channels. In group 1, the activation under MI+AO condition for all channels was the best. In group 2, the activation under the AO condition was the best.

B. Average ERD Value

In order to investigate the differences in the EEG response characteristics of the same group under different experimental conditions, we calculated the subjects' average ERD values in four frequency bands separately, and the average ERD values under different experimental conditions were subjected to paired t-test. Fig. 3 represents the average ERD values of the two groups of subjects under different experimental conditions in the four frequency bands, and the involved channels include C3, FC3 and CP3.

The average ERD values in group 1 are shown in Fig. 3(a). It could be found that in the low alpha frequency band, the average ERD value under MI+AO condition was stronger than that under AO condition, and the average ERD value under MI condition was weaker than that under AO condition for C3 or CP3 channels. In addition, the value under the AO condition of FC3 channel is positive, which is due to the individual difference, so the low alpha band sometimes has an increase in energy. In the low beta frequency band, the average ERD values under different experimental conditions were ranked as: MI+AO>AO>MI, and in channel CP3, the average ERD value under MI+AO condition was statistically significantly different from that under AO ($p = 0.0222 < 0.05$) or MI ($p = 0.0129 < 0.05$) conditions.

The average ERD values in group 1 are shown in Fig. 3(a). It could be found that in the low alpha frequency band, the

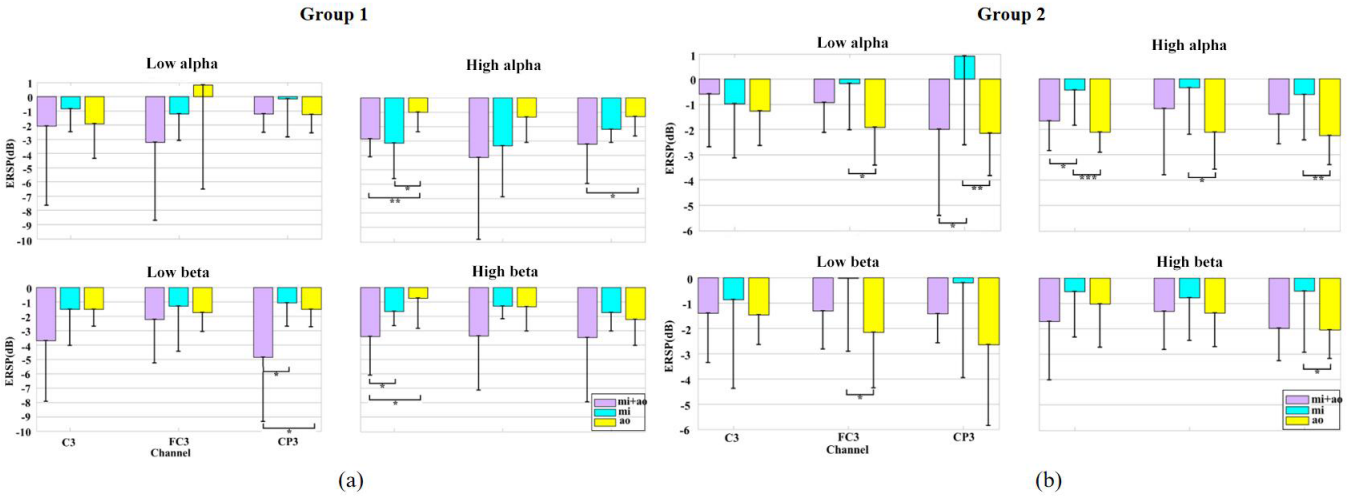

Fig. 3. (a) Average ERD values of group 1 subjects in the four frequency bands under different experimental conditions. (b) Average ERD values of group 2 subjects in the four frequency bands under different experimental conditions. All subplots have the same scale as the first subplot in the second row. Statistical differences are marked by asterisks, one star indicates $p < 0.05$, two stars indicate $p < 0.01$, and three stars indicate $p < 0.001$.

average ERD value under MI+AO condition was stronger than that under AO condition, and the average ERD value under MI condition was weaker than that under AO condition for C3 or CP3 channels. In addition, the value under the AO condition of FC3 channel is positive, which is due to the individual difference, so the low alpha band sometimes has an increase in energy. In the low beta frequency band, the average ERD values under different experimental conditions were ranked as: MI+AO>AO>MI, and in channel CP3, the average ERD value under MI+AO condition was statistically significantly different from that under AO ($p = 0.0222 < 0.05$) or MI ($p = 0.0129 < 0.05$) conditions.

In the high alpha band, the averageERD value under MI+AO or MI conditions was stronger than that under AO condition, and in channels C3 or CP3, the average ERD value under MI+AO condition was statistically significantly different from that under AO condition (C3: $p = 0.0020 < 0.01$, CP3: $p = 0.0399 < 0.05$). In the high beta band, the average ERD under MI+AO condition was stronger than that under AO or MI conditions, and in channel C3, the average ERD value under MI+AO condition was statistically significantly different from that under AO ($p = 0.0129 < 0.05$) or MI ($p = 0.0457 < 0.05$) conditions.

The results presented in the histogram were consistent with those presented in the ERSP time-frequency diagram, i.e., AO better elicited sensorimotor cortex activation in the low alpha and low beta frequency bands, while MI better elicited activation in the high alpha and high beta frequency bands, and the MI+AO condition had the best sensorimotor cortex activation in the subjects.

The average ERD values in group 2 are shown in Fig. 3(b). In the low alpha band, the average ERD value in channel FC3 under AO condition was stronger than that under MI condition and statistically significantly different. In the channel CP3, the average ERD value under MI condition was significantly weaker than that under MI+AO ($p = 0.0353 < 0.05$) or AO ($p = 0.0073 < 0.01$) conditions. In the low beta band, the average ERD values under different experimental conditions were ordered as AO>MI+AO>MI, and in the FC3 channel, the average ERD value under AO condition was statistically significantly different from that under MI condition ($p = 0.0371 < 0.01$).

As in the low beta band, the average ERD values under different experimental conditions were ordered as AO>MI+AO>MI in the high alpha band. And for all channels, there was a statistically significant difference in average ERD values between the AO condition and the MI condition (C3: $p = 7.2061e\text{-}4 < 0.001$, FC3: $p = 0.0101 < 0.05$, CP3: $p = 0.0095 < 0.01$). In the channel C3, the average ERD value under the MI condition was also statistically significantly different from that under MI+AO condition ($p = 0.0190 < 0.05$). In the high beta band, for all channels, the weakest average ERD value was found in the MI condition. And in the channel CP3, there was a statistically significant difference in average ERD values between the AO condition and the MI condition ($p = 0.0412 < 0.05$). Overall, the ERD phenomenon under the AO condition was the most obvious and significantly stronger than that under the MI condition.

To investigate the differences of EEG response characteristics in different groups under the same experimental conditions, we calculated the average ERD values of the two groups in the four frequency bands respectively, and performed independent sample t-test on the average ERD values of the two groups under the same experimental conditions. Fig. 4 shows the average ERD values of the two groups in the four frequency bands under the three experimental conditions.

Under the MI+AO condition, the average ERD values were higher in group 1 than in group 2 in all frequency bands and channels except CP3 channel in low alpha band. And in C3 ($p = 0.0118 < 0.05$), CP3 ($p = 0.0312 < 0.05$) channels in the high alpha band, and CP3 channel in the low beta band

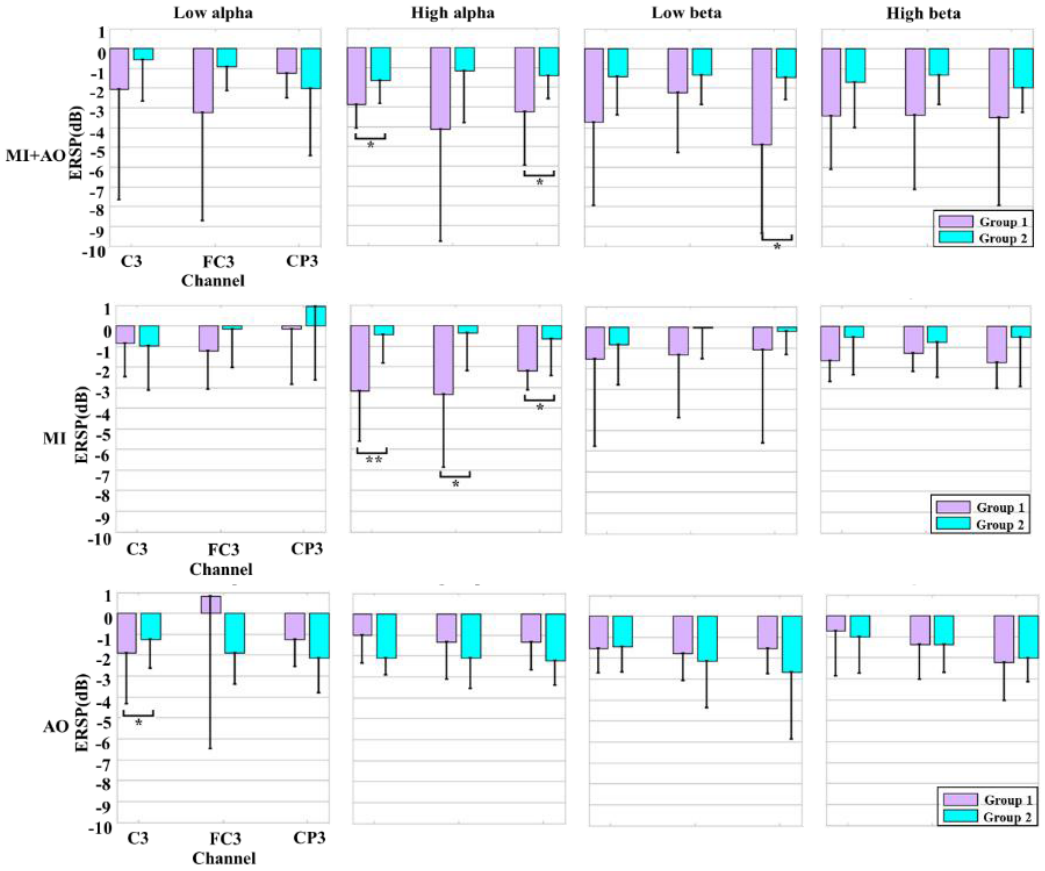

Fig. 4. Mean ERD values of the two groups of subjects in the four frequency bands under the three experimental conditions. All subplots have the same scale as the first subplot in the first row. Statistical differences are marked by asterisks, one star indicates $p < 0.05$ and two stars indicate $p < 0.01$.

($p = 0.0115 < 0.05$), there was a statistically significant difference in average ERD values between group 1 and group 2.

Under the MI condition, except for the C3 channel in the low alpha band, all other bands and channels had higher average ERD values in group 1 than in group 2. In all channels in the high alpha band (C3:$p = 0.0017 < 0.01$, CP3:$p = 0.0112 < 0.05$, FC3:$p = 0.0117 < 0.05$), there was a statistically significant difference in average ERD values between group 1 and group 2.

Under the AO condition, the average ERD values were stronger in group 2 than in group 1 in all bands and channels except for the C3 channel in low alpha and the CP3 channel in high beta band, and there was a statistically significant difference between the two groups in C3 channel in high alpha band ($p = 0.0117 < 0.05$). This is consistent with the results presented by the time-frequency diagram, that is, under all experimental conditions involving MI, the overall ERD intensity in group 1 is stronger than that in group 2. This is also a good evidence of the disparity in the level of MI between the two groups.

C. Brain Topography

Fig. 5 represents the average brain topography in the two groups in the four frequency bands under different experimental conditions. In group 1, it could be found that the activation under the MI condition was concentrated in the sensorimotor cortex and showed a contralateral dominance, while the activation of sensorimotor cortex under the MI+AO condition was higher than that under the MI condition and also showed contralateral dominance in the high alpha and high beta frequency bands. In group 2, subjects had almost no activation of sensorimotor cortex under the MI condition, and had activation of sensorimotor cortex under AO and MI+AO conditions but did not show contralateral predominance. The intensity and range of activation in the cortex of group 1 subjects were stronger than those of group 2 in all four frequency bands under the same experimental conditions.

D. Brain Network and Its Parameters

In order to show the causal interaction between channels more clearly, the amount of effective connections was limited by setting a threshold of 60% of the maximum PDC value of each subject. In addition, the statistical significance (unilateral t-test, $p < 0.01$) of non-zero PDC values was assessed by means of a bootstrap approach using phase randomization according to the Theiler's method. Fig. 6 shows the brain network diagrams of the two groups under different experimental conditions. In group 1, all three experimental conditions involved sensorimotor and visual-related channels, and the MI+AO condition contained the most "target" nodes and concentrated in the sensorimotor cortex. In group 2, the "target" nodes in the MI+AO condition were CP6, P3, P5,

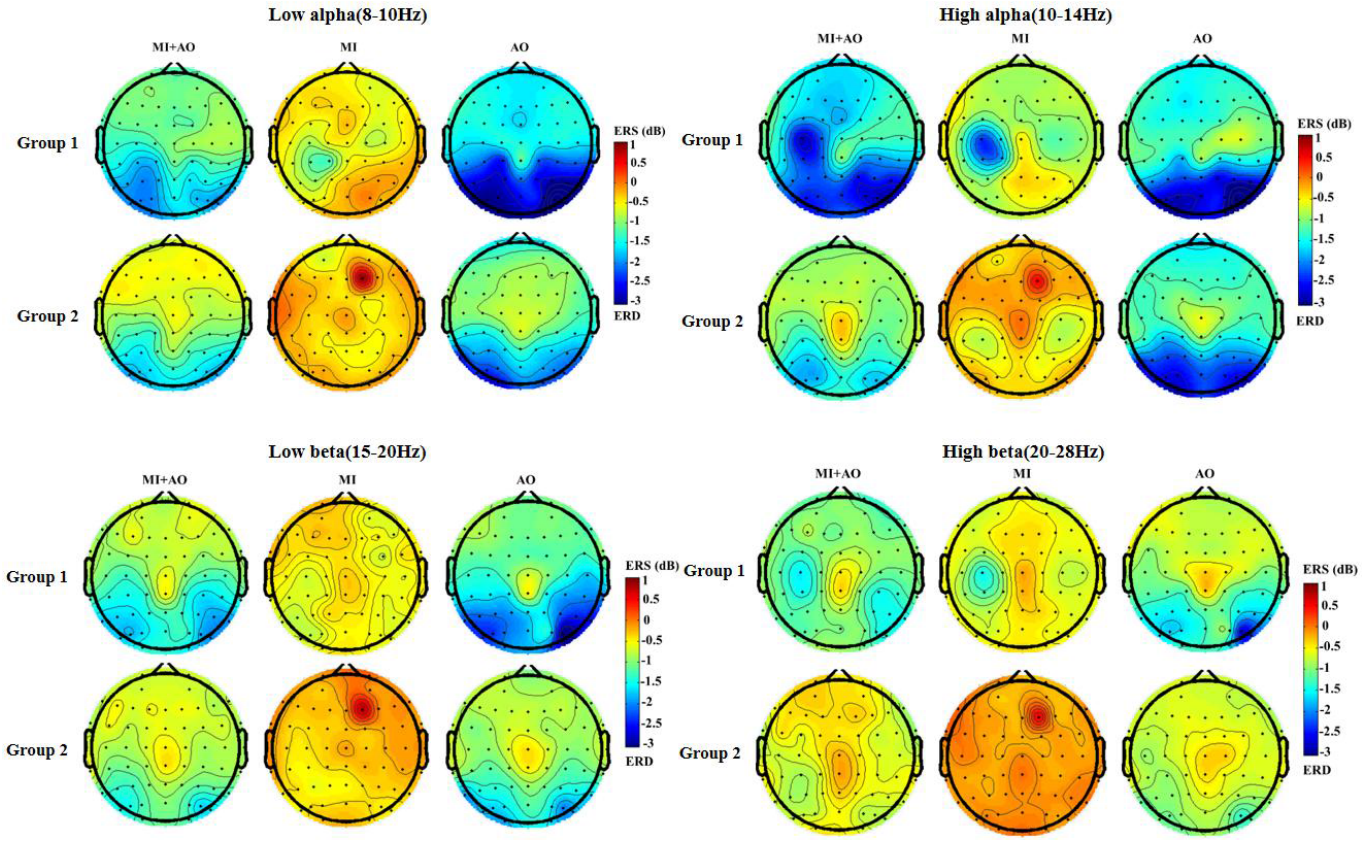

Fig. 5. Mean brain topography of two groups of subjects in the four frequency bands under the three experimental conditions.

P6, and PO3 channels, which were mainly distributed in the sensory and visual-related cortices. The "target" nodes in the AO condition involved more channels in the sensorimotor cortex. The number of network information flows in the MI condition was significantly lower than that in the other conditions.

Fig.7 shows the causal flow diagrams of 20 channels for the two groups under different experimental conditions. Combining the brain network diagrams and the causal flow diagrams, we can find that the causal flow of the "source" node ranges from 0 to 9, and the distribution is more uniform in the cortex, while the causal flow value of the "target" node was larger and only existed in a few channels. In group 1, most of the "source" nodes had higher causal flow values than the other two conditions under the MI+AO condition. In group 2, the causal flow value of most "source" nodes in the AO condition was higher than that in the MI+AO condition. Therefore, the information transmission capacity of the sensorimotor cortical network was stronger under the MI+AO condition for subjects in group 1, whereas the information transmission capacity was stronger under the AO condition for subjects in group 2.

E. Classification Accuracy

The classification results are shown in Fig. 8,with an average classification accuracy of 76.63% for group 1 subjects and 67.22% for group 2 subjects. The results of the statistical t-test showed that there was a significant difference in classification accuracy between group 1 and group 2 ($p = 0.0434 < 0.05$). Sjoerd D V et al. used patient MI accuracy as a basis for judging the recovery of MI ability after stroke in a study [38]. Morris T et al. suggested that the accuracy of MI could be used to reflect how well subjects had MI [39]. Vuckovic A et al. attempted to predict subjects' MI-BCI performance by the MI questionnaire and showed a correlation between the accuracy of the BCI classification and the results of the MI questionnaire [40]. Thus this result again validates that there is a difference between the two groups in terms of MI levels.

IV. Discussion

The results of the time-frequency analysis showed that under the MI, MI+AO condition, i.e. the experimental condition with MI participation, the energy drop in the sensorimotor cortex in group 1 was stronger than that in group 2 under the same conditions. The analysis of brain networks and their parameters also showed relevant results, i.e., the brain network functional connectivity of group 1 under MI or MI+AO conditions were stronger than those of group 2. In addition, MI classification accuracy was also significantly higher in group 1 subjects than in group 2. The above findings demonstrate that the MI level of group 1 subjects was stronger than that of group 2. Therefore, we believe that the reason for the difference in cortical activation between different subjects under MI and AO conditions may be the subject's MI level. It is noteworthy that the performance of group 1 was weaker than that of group 2 under the AO condition, which may be due to the fact that people with weak MI EEG features are more likely to induce imitation of movements in the cerebral cortex during AO.

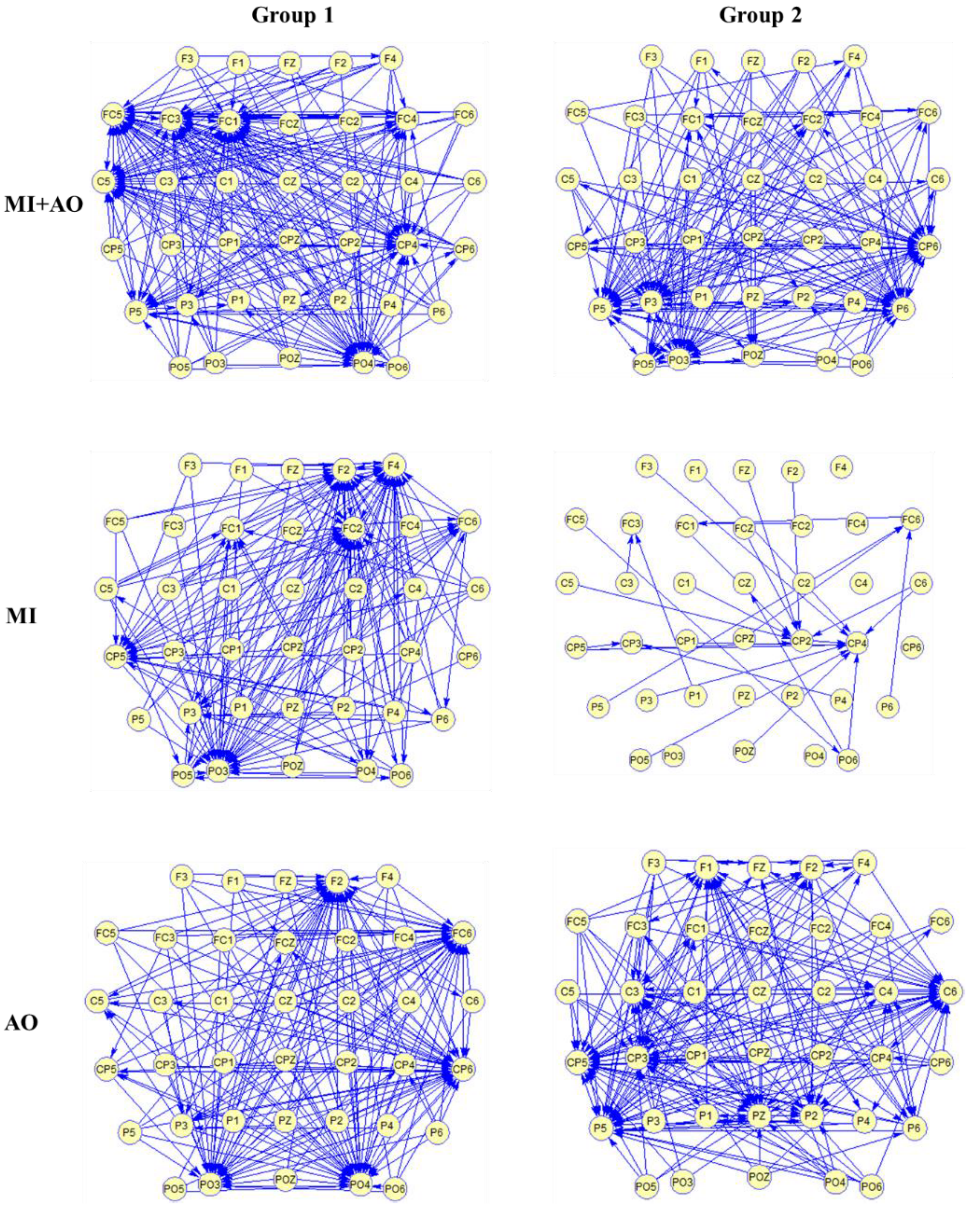

Fig. 6. Brain network maps of two groups of subjects under different experimental conditions.

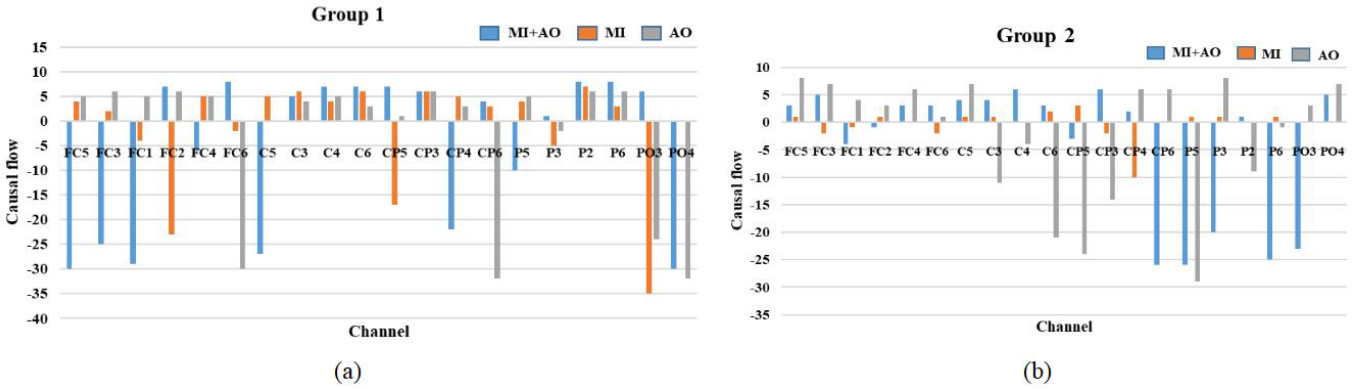

Fig. 7. (a) Flow diagram of causality corresponding to each channel in group 1 subjects under different experimental conditions. (b) Flow diagram of causality corresponding to each channel in group 2 subjects under different experimental conditions.

In the analysis of the average ERD energy map, AO elicited better activation of sensorimotor cortex in the low alpha and low beta frequency bands and MI elicited better activation in the high alpha and high beta frequency bands in the C3 channel of group 1. This may be because the widespread low alpha and low beta desynchronization is associated with increased

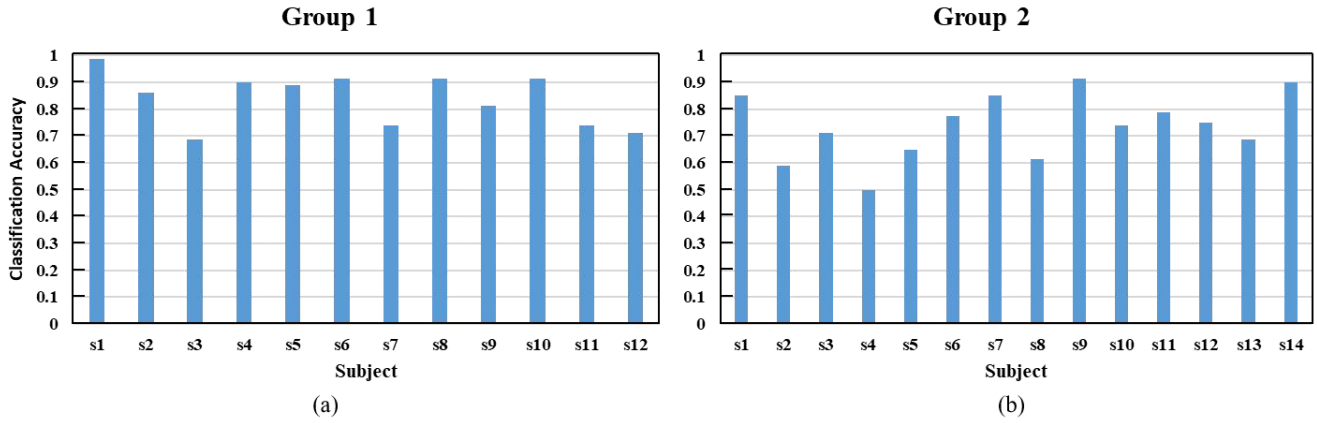

Fig. 8. (a) Correct classification rate of MI state and resting state in group 1 subjects. (b) Correct classification rate of MI state and resting state in group 2 subjects.

levels of attention and arousal of the motor system during motor execution and action observation. In contrast, high alpha and beta band desynchronization reflects the activation of neural circuits associated with individual processing of motor commands and somatosensory and visual feedback during motor execution and observation, with motor specificity.

In group 1, the activation effect of the MI+AO condition was the best in the sensorimotor cortex, which might be because AO has a certain role in guiding and improving attention compared with pure MI. In group 2, the activation effect of AO condition was the best in sensorimotor cortex, while MI+AO was slightly weaker than AO. This may be because the MI during the AO process will occupy a part of the subject's attention, but the subject is not skilled or even knows how to perform the MI, thus affecting the activation effect of the cortex.

We found the general trend that "the two groups of people showed opposite differences in cortical activation under MI and AO conditions". Based on this trend, it is reasonable to assume that "different motor evoked paradigms are applicable to different populations". Therefore, subjects were divided into two groups based on the comparison of activation intensity in sensorimotor cortex under MI and AO conditions. And then the EEG responses of cortex under the same evoked paradigm between groups and different motor evoked paradigms within groups were explored. The inter-group results verified the rationality and feasibility of grouping. The intra-group results proved that different groups were suitable for different motor evoked paradigms, which proved the effectiveness of grouping. These results provide preliminary evidence of the rationality of grouping and provide ideas for future related studies.

V. Conclusion

We grouped the subjects according to the relative ERD energy values in the high alpha band of channel C3 under MI and AO conditions, and analyzed the two groups of subjects by time-frequency maps, average ERD energy, brain topography, and classification accuracy. The EEG activations of subjects under MI+AO, MI, AO three experimental conditions revealed the difference law of the opposite cortical activation of the two groups under MI and AO conditions, and proposed that motor evoked paradigms that can effectively activate the cortex in two groups of people, which is expected to provide stroke patients with a motor evoked paradigm with individual applicability, and provide key technical support for optimizing the rehabilitation process and treatment effect.

Acknowledgment

The authors would like to thank all participants for their voluntary participation.

References

[1] M.-Z. Yuan et al., "Research on the cause of death for severe stroke patients," *J. Clin. Nursing*, vol. 27, nos. 1–2, pp. 450–460, Jan. 2018.

[2] M. Y. Hathidara, V. Saini, and A. M. Malik, "Stroke in the young: A global update," *Current Neurol. Neurosci. Rep.*, vol. 19, no. 11, pp. 1–8, Nov. 2019.

[3] S. Wu et al., "Stroke in China: Advances and challenges in epidemiology, prevention, and management," *Lancet Neurol.*, vol. 18, no. 4, pp. 394–405, 2019.

[4] G. Kwakkel, B. J. Kollen, J. Van Der Grond, and A. J. H. Prevo, "Probability of regaining dexterity in the flaccid upper limb: Impact of severity of paresis and time since onset in acute stroke," *Stroke*, vol. 34, no. 9, pp. 2181–2186, Sep. 2003.

[5] A. Basteris and M. N. Sharon, "Training modalities in robot-mediated upper limb rehabilitation in stroke: A framework for classification based on a systematic review," *J. Neuroeng. Rehabil.*, vol. 11, no. 1, pp. 111–125, 2014.

[6] P. Langhorne, F. Coupar, and A. Pollock, "Motor recovery after stroke: A systematic review," *Lancet Neurol.*, vol. 8, no. 8, pp. 741–754, Aug. 2009.

[7] S. M. Hatem et al., "Rehabilitation of motor function after stroke: A multiple systematic review focused on techniques to stimulate upper extremity recovery," *Frontiers Hum. Neurosci.*, vol. 10, p. 442, Sep. 2016.

[8] K. N. Arya, R. Verma, R. K. Garg, V. P. Sharma, M. Agarwal, and G. G. Aggarwal, "Meaningful task-specific training (MTST) for stroke rehabilitation: A randomized controlled trial," *Topics Stroke Rehabil.*, vol. 19, no. 3, pp. 193–211, May 2012.

[9] J. A. Kleim, T. A. Jones, and T. Schallert, "Motor enrichment and the induction of plasticity before or after brain injury," *Neurochemical Res.*, vol. 28, pp. 1757–1769, Nov. 2003.

[10] A. Flöel et al., "Physical fitness training in subacute stroke (PHYS-STROKE)—Study protocol for a randomised controlled trial," *Trials*, vol. 15, no. 1, pp. 1–12, Dec. 2014.

[11] S. Sutbeyaz, G. Yavuzer, N. Sezer, and B. F. Koseoglu, "Mirror therapy enhances lower-extremity motor recovery and motor functioning after stroke: A randomized controlled trial," *Arch. Phys. Med. Rehabil.*, vol. 88, no. 5, pp. 555–559, May 2007.

[12] P. W. Duncan, "Synthesis of intervention trials to improve motor recovery following stroke," *Topics Stroke Rehabil.*, vol. 3, no. 4, pp. 1–20, Jan. 1997.
[13] K. Wang, Z. Wang, W. Ren, and C. Yang, "Design of sports rehabilitation training system based on EEMD algorithm," *Comput. Intell. Neurosci.*, vol. 2022, pp. 1–10, Jun. 2022.
[14] N. A. Bayona, J. Bitensky, K. Salter, and R. Teasell, "The role of task-specific training in rehabilitation therapies," *Topics Stroke Rehabil.*, vol. 12, no. 3, pp. 58–65, Jul. 2005.
[15] S. C. Cramer, "Repairing the human brain after stroke: I. Mechanisms of spontaneous recovery," *Ann. Neurol.*, vol. 63, no. 3, pp. 272–287, Mar. 2008.
[16] M. A. Dimyan and L. G. Cohen, "Neuroplasticity in the context of motor rehabilitation after stroke," *Nature Rev. Neurol.*, vol. 7, no. 2, pp. 76–85, Feb. 2011.
[17] M. Van Gerven et al., "The brain-computer interface cycle," *J. Neural Eng.*, vol. 6, no. 4, 2009, Art. no. 041001.
[18] K. Shibata, T. Watanabe, Y. Sasaki, and M. Kawato, "Perceptual learning incepted by decoded fMRI neurofeedback without stimulus presentation," *Science*, vol. 334, no. 6061, pp. 1413–1415, Dec. 2011.
[19] S. Silvoni et al., "Brain-computer interface in stroke: A review of progress," *Clin. EEG Neurosci.*, vol. 42, no. 4, pp. 245–252, Oct. 2011.
[20] R. Mane, T. Chouhan, and C. Guan, "BCI for stroke rehabilitation: Motor and beyond," *J. Neural Eng.*, vol. 17, no. 4, Aug. 2020, Art. no. 041001.
[21] F. Cincotti et al., "EEG-based brain-computer interface to support post-stroke motor rehabilitation of the upper limb," in *Proc. Annu. Int. Conf. IEEE Eng. Med. Biol. Soc.*, Sep. 2012, pp. 4112–4115.
[22] N. Sharma, V. M. Pomeroy, and J.-C. Baron, "Motor imagery: A backdoor to the motor system after stroke?" *Stroke*, vol. 37, no. 7, pp. 1941–1952, Jul. 2006.
[23] M. Rensink, M. Schuurmans, E. Lindeman, and T. Hafsteinsdottir, "Task-oriented training in rehabilitation after stroke: Systematic review," *J. Adv. Nursing*, vol. 65, no. 4, pp. 737–754, 2009.
[24] M. Jeannerod and V. Frak, "Mental imaging of motor activity in humans," *Current Opinion Neurobiol.*, vol. 9, no. 6, pp. 735–739, Dec. 1999.
[25] J. Munzert, B. Lorey, and K. Zentgraf, "Cognitive motor processes: The role of motor imagery in the study of motor representations," *Brain Res. Rev.*, vol. 60, no. 2, pp. 306–326, May 2009.
[26] A. M. Bruton, P. S. Holmes, D. L. Eaves, Z. C. Franklin, and D. J. Wright, "Neurophysiological markers discriminate different forms of motor imagery during action observation," *Cortex*, vol. 124, pp. 119–136, Mar. 2020.
[27] R. Gatti, A. Tettamanti, P. M. Gough, E. Riboldi, L. Marinoni, and G. Buccino, "Action observation versus motor imagery in learning a complex motor task: A short review of literature and a kinematics study," *Neurosci. Lett.*, vol. 540, pp. 37–42, Apr. 2013.
[28] W. Taube, M. Mouthon, C. Leukel, H.-M. Hoogewoud, J.-M. Annoni, and M. Keller, "Brain activity during observation and motor imagery of different balance tasks: An fMRI study," *Cortex*, vol. 64, pp. 102–114, Mar. 2015.
[29] S. Clark, F. Tremblay, and D. Ste-Marie, "Differential modulation of corticospinal excitability during observation, mental imagery and imitation of hand actions," *Neuropsychologia*, vol. 42, no. 1, pp. 105–112, Jan. 2004.
[30] A. Delorme and S. Makeig, "EEGLAB: An open source toolbox for analysis of single-trial EEG dynamics including independent component analysis," *J. Neurosci. Methods*, vol. 134, no. 1, pp. 9–21, Mar. 2004.
[31] R. Grandchamp and A. Delorme, "Single-trial normalization for event-related spectral decomposition reduces sensitivity to noisy trials," *Frontiers Psychol.*, vol. 2, p. 236, 2011.
[32] C. Babiloni et al., "Alpha, beta and gamma electrocorticographic rhythms in somatosensory, motor, premotor and prefrontal cortical areas differ in movement execution and observation in humans," *Clin. Neurophysiol.*, vol. 127, no. 1, pp. 641–654, Jan. 2016.
[33] C. Neuper, R. Scherer, M. Reiner, and G. Pfurtscheller, "Imagery of motor actions: Differential effects of kinesthetic and visual–motor mode of imagery in single-trial EEG," *Cognit. Brain Res.*, vol. 25, no. 3, pp. 668–677, Dec. 2005.
[34] C. Neuper and G. Pfurtscheller, "Motor imagery and ERD," in *Handbook of Electroencephalography and Clinical Neurophysiology*, vol. 6. Amsterdam, The Netherlands: Elsevier, 1999, pp. 305–325.
[35] Y. Jeon, C. S. Nam, Y.-J. Kim, and M. C. Whang, "Event-related (De)synchronization (ERD/ERS) during motor imagery tasks: Implications for brain-computer interfaces," *Int. J. Ind. Ergonom.*, vol. 41, no. 5, pp. 428–436, Sep. 2011.
[36] C. J. Stam, "From synchronisation to networks: Assessment of functional connectivity in the brain," in *Coordinated Activity in the Brain*. New York, NY, USA: Springer, 2009, pp. 91–115.
[37] L. A. Baccalá and K. Sameshima, "Partial directed coherence: A new concept in neural structure determination," *Biol. Cybern.*, vol. 84, no. 6, pp. 463–474, May 2001.
[38] S. de Vries, M. Tepper, B. Otten, and T. Mulder, "Recovery of motor imagery ability in stroke patients," *Rehabil. Res. Pract.*, vol. 2011, pp. 1–9, 2011.
[39] T. Morris, S. Michael, and A. P. Watt, *Imagery in Sport*. Champaign, IL, USA: Human Kinetics, 2005.
[40] A. Vuckovic and B. A. Osuagwu, "Using a motor imagery questionnaire to estimate the performance of a brain-computer interface based on object oriented motor imagery," *Clin. Neurophysiol.*, vol. 124, no. 8, pp. 1586–1595, Aug. 2013.